GULF RADIATION TECHNOLOGY

GA-10344

RADIATION EFFECTS IN SILICON SOLAR CELLS

Quarterly Progress Report
Covering the Period 1 July through 30 September 1970

R. A. Berger, J. F. Colwell, R. E. Leadon,
J. A. Naber, B. C. Passenheim

Jet Propulsion Laboratory
Contract 952387
Gulf Radiation Technology Project 6105

October 10, 1970

GULF RADIATION TECHNOLOGY, A DIVISION OF GULF ENERGY & ENVIRONMENTAL SYSTEMS, INC., P.O. BOX 608, SAN DIEGO, CALIFORNIA 92112

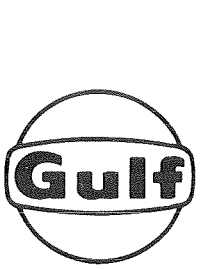

GULF RADIATION TECHNOLOGY

GA-10344

RADIATION EFFECTS IN SILICON SOLAR CELLS

Quarterly Progress Report
Covering the Period 1 July through 30 September 1970

R. A. Berger, J. F. Colwell, R. E. Leadon,
J. A. Naber, B. C. Passenheim

Jet Propulsion Laboratory
Contract 952387
Gulf Radiation Technology Project 6105

October 10, 1970

GULF RADIATION TECHNOLOGY, A DIVISION OF GULF ENERGY & ENVIRONMENTAL
SYSTEMS, INC., P.O. BOX 608, SAN DIEGO, CALIFORNIA 92112

CONTENTS

1. INTRODUCTION

The overall purpose of this program is to ascertain the nature of the defects responsible for the degradation in output of silicon devices (solar cells) irradiated by space radiation. When the nature of the defects and their annealing mechanisms are known, it will be possible (1) to determine the parameters that will lead to development of radiation-hardened devices, (2) to predict the effects of radiation and annealing on solar cells, and (3) to make use of computer programs to predict radiation effects in solar cells on extended space flights.

The present effort is concentrated on the study of the effects of lithium on the production and annealing of damage in silicon. This work is being performed on lithium-diffused bulk silicon using measurements such as minority-carrier lifetime, electron-spin resonance (ESR), electrical conductivity, and infrared absorption. The temperature range from 77.5° to 400°K is under investigation. The damage is introduced by 30-MeV electrons and fission neutrons.

2. TECHNICAL DISCUSSION

2.1 MINORITY-CARRIER LIFETIME

During this quarter, minority-carrier lifetime studies have been performed on 30-MeV electron-irradiated lithium-diffused high-purity quartz-crucible (QC) silicon. A 60-ohm-cm silicon boule was purchased from Wacker Chemical Company.

Figure 1 shows the minority-carrier lifetime temperature dependence of the starting material. This temperature dependence indicates recombination due to about 4×10^{10}/cc attractive centers farther than 0.4 eV from a band edge.[1] Two-millimeter-thick slices of silicon were lithium-diffused by the lithium-oil paint-on technique and redistributed to a uniform donor density of about 2×10^{15}/cc, as determined by resistivity[2] and Hall effect measurements. The resistivity of these samples was about 2 ohm-cm.

That the 60-ohm-cm material actually contained oxygen was verified by infrared absorption measurements of the 9-μm absorption band due to oxygen.[3] Only a small 9-μm lattice band was observed in the 10^4-ohm-cm and 0.4-ohm-cm float-zone (FZ) silicon previously used in lifetime and ESR measurements.

Figure 2 shows a family of curves of minority-carrier lifetime for the 2-ohm-cm lithium-diffused QC silicon versus temperature including preirradiation, postirradiation, and postirradiation-postanneal measurements. These lifetime temperature dependences can be attributed to recombination through attractive centers more than 0.35 eV from a band edge. If the capture cross sections of Lax[1] are used, the preirradiation lifetime indicates about 6×10^{10} centers/cc, rising to about 5×10^{11} centers/cc after irradiation to a fluence of 2.6×10^{12} e/cm^2 and dropping to about 1.2×10^{11}/cc after a 25-minute anneal at 385°K. For the sample shown in Fig. 2, the room temperature minority-carrier lifetime degradation constant was found to be $K = 3.9 \pm 0.3 \times 10^{-8}$ cm^2/e-sec, which is comparable to both diffused and non-diffused silicon of similar resistivity.

Figure 3 is a plot of inverse lifetime versus fluence for another 2-ohm-cm sample, showing 300°K lifetime degradation and anneal. For this

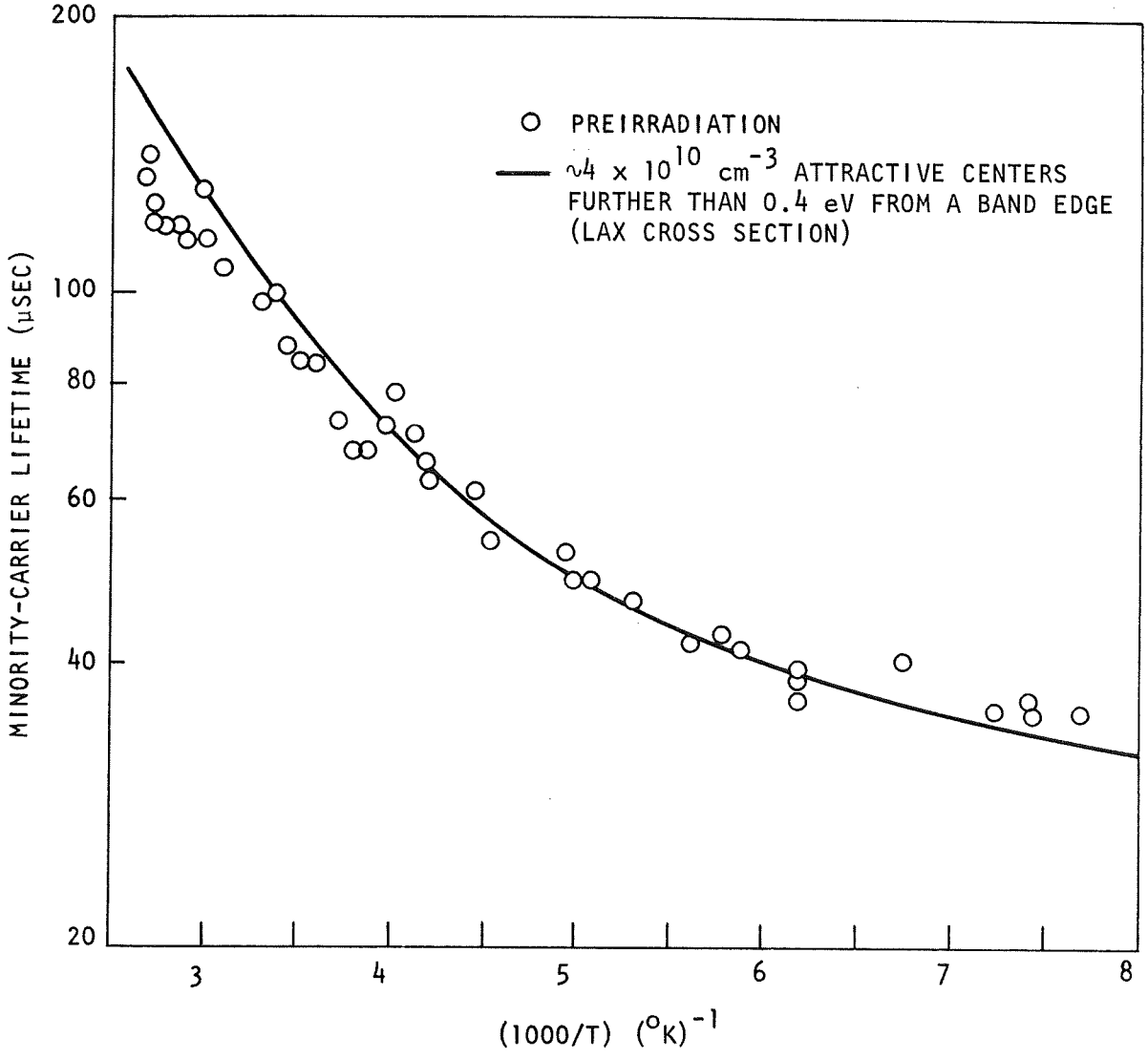

Fig. 1. Temperature dependence of minority-carrier lifetime for 60-ohm-cm quartz-crucible silicon (not lithium-diffused)

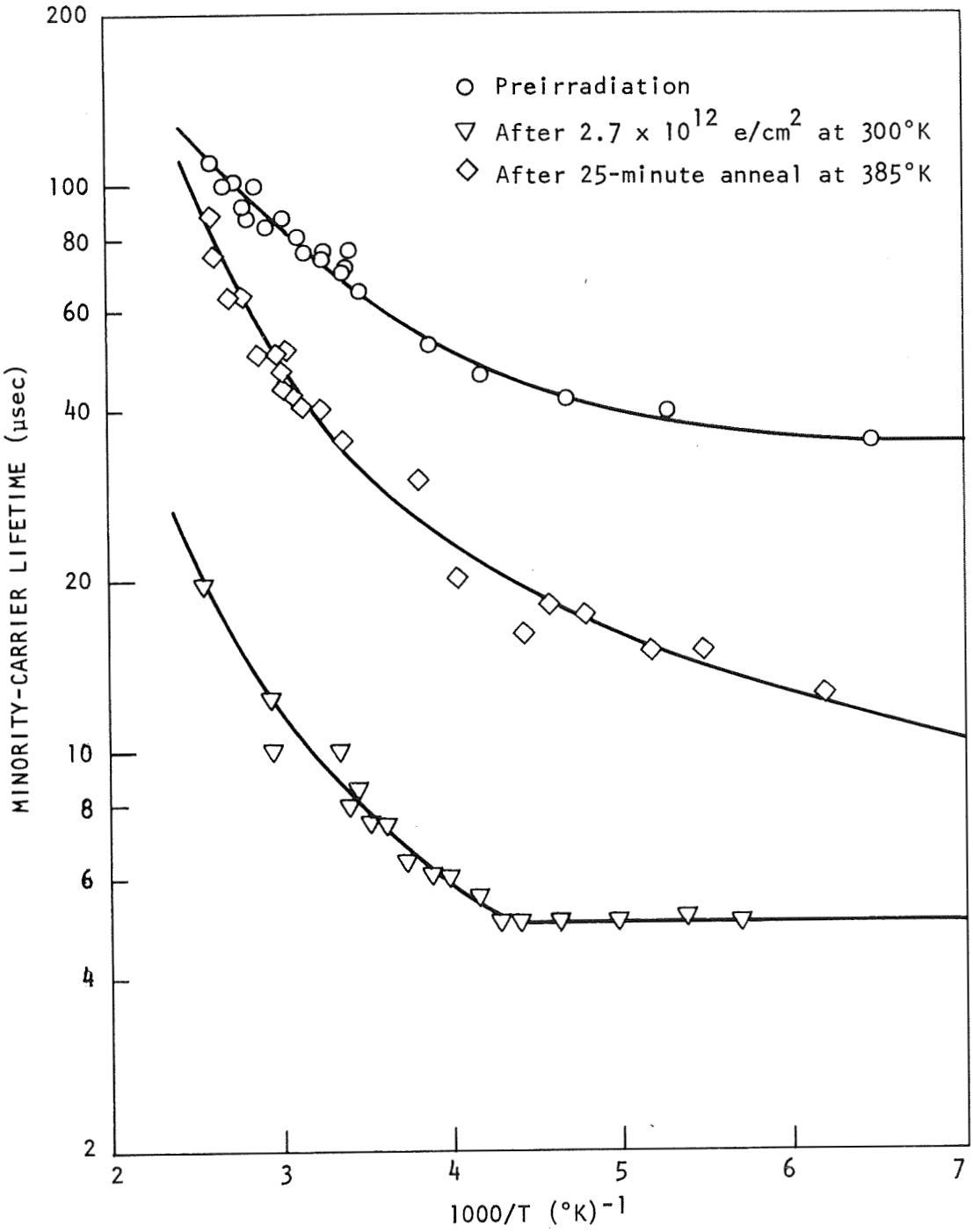

Fig. 2. Temperature dependence of minority-carrier lifetime for a 2-ohm-cm lithium-diffused quartz-crucible silicon sample, before and after irradiation with 2.7 x 10^{12} e/cm^2 30-MeV electrons at 300°K and after a 25-minute anneal at 385°K

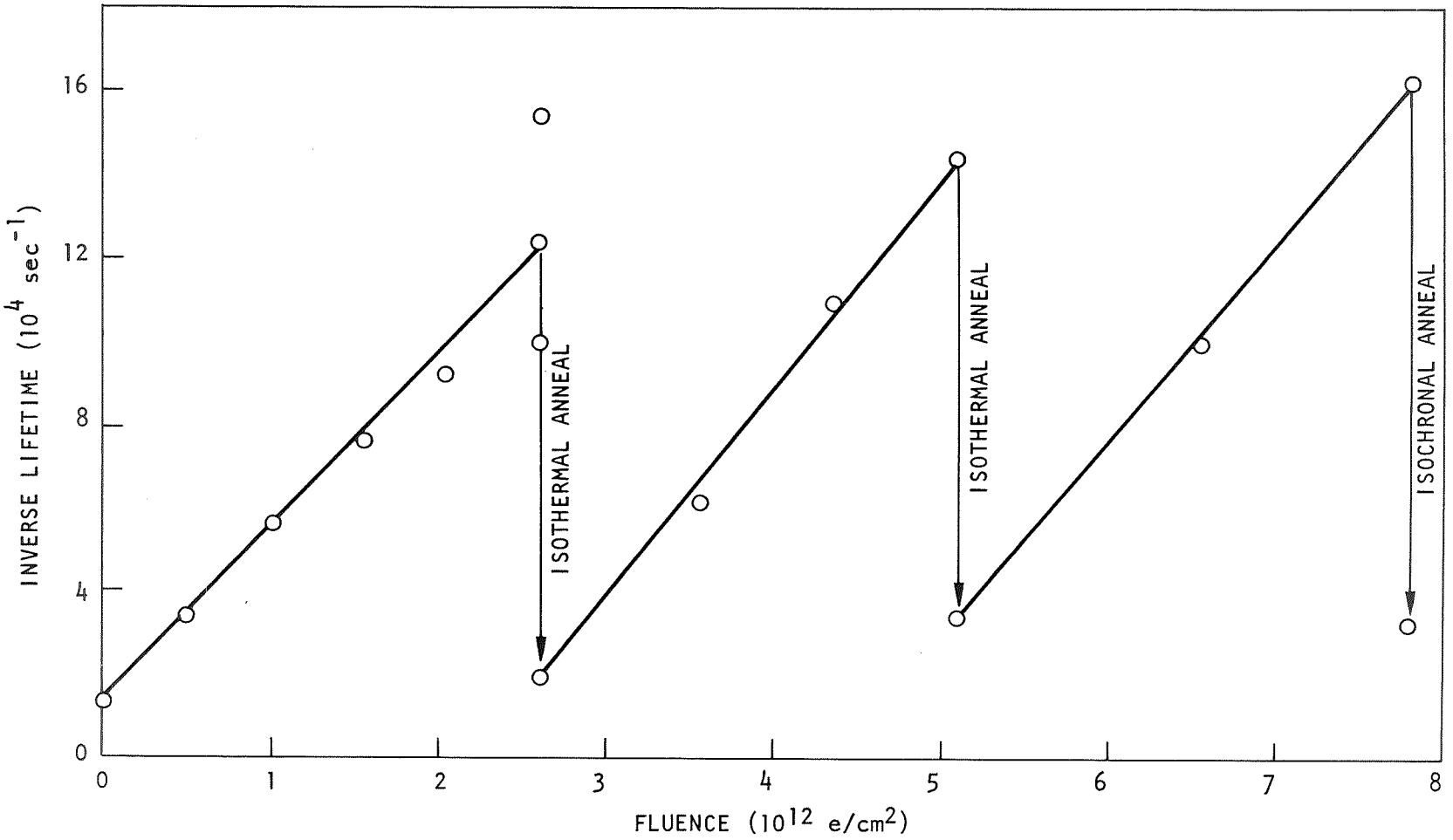

Fig. 3. Inverse minority-carrier lifetime versus 30-MeV electron fluence for a 2-ohm-cm quartz-crucible silicon sample irradiated at 300°K; isochronal annealed at 385° to 390°K for 25 to 30 minutes

sample, the degradation constant was $K = 4.5 \pm 0.3 \times 10^{-8}$ cm^2/e-sec. One sample was also irradiated at 112° and 217°K.

Figure 4 shows the minority-carrier lifetime temperature dependence before and after irradiation at 112°K. Also shown is the lifetime temperature dependence after a 30-minute, 390°K anneal. Again, the lifetime temperature dependence can be attributed to attractive deep recombination centers. From these measurements, a defect center introduction rate of 0.15 cm^{-1} is estimated, if Lax's cross section[1] is assumed, for irradiations with 30-MeV electrons at all temperatures between 100° and 300°K. To determine the annealing behavior of these samples, both isochronal and isothermal anneals were performed after room-temperature irradiation.

Figure 5 shows a family of curves representing the unannealed fraction of annealable defects versus anneal time for isothermal anneals at 385°, 395°, and 411°K. Figure 6 shows the unannealed fraction of annealable defects versus anneal temperature for 5-minute isochronal anneals. In these plots, the defect density is taken to be inversely proportional to the minority-carrier lifetime. Isochronal anneals are centered near 375°K, and isochronal and isothermal anneals indicate an activation energy for anneal of about 0.65 ± 0.20 eV. This activation energy is less than the 1.1 eV anticipated for lithium diffusion in oxygen-containing silicon, even though infrared absorption measurements show the material does contain considerable oxygen. Since there is considerable experimental uncertainty in our annealing results, additional annealing measurements are planned.

It is very interesting that the minority-carrier lifetime shows no evidence of the Si-Bl (oxygen-vacancy) center, although electron-spin resonance measurements[4] on a comparable lithium-diffused quartz-crucible sample (10^{16} Li/cc) indicate an introduction rate of about 0.15 cm^{-1} after a 30-MeV electron fluence of 5×10^{16} e/cm^2. If silicon Si-Bl centers were produced at that rate, their effect on the minority-carrier lifetime should be readily apparent at temperatures below about 200°K. Thus, the present measurements indicate the Si-Bl center introduction rate in these samples has been reduced by the presence of lithium.

A possible explanation for this is that the radiation-induced mobile vacancies, which are negatively charged in n-type silicon, are captured by

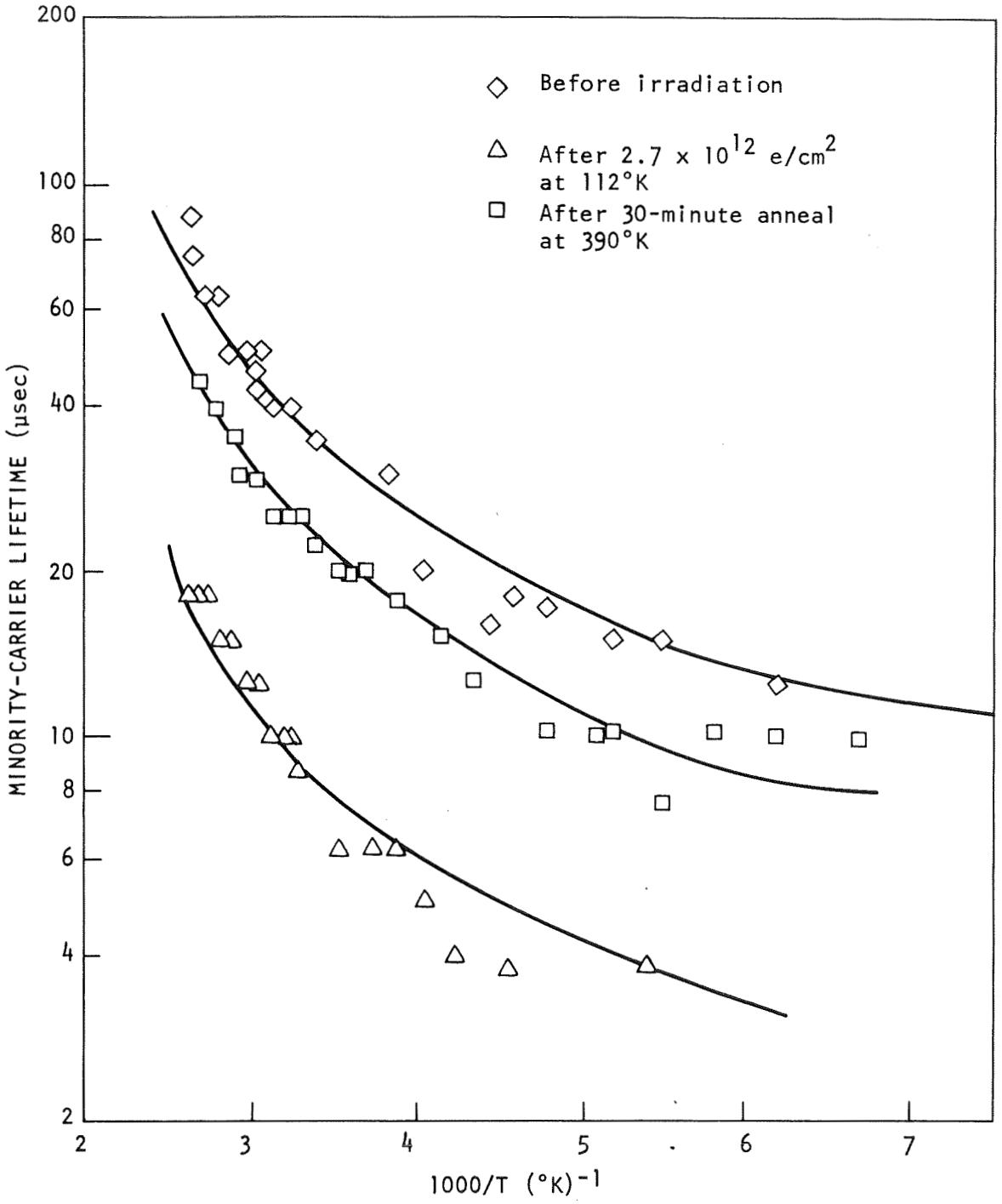

Fig. 4. Temperature dependence of minority-carrier lifetime for a 2-ohm-cm oxygen-containing lithium-diffused silicon sample, before and after irradiation with 2.7 x 10^{12} e/cm^2 30-MeV electrons at 112°K, and after a 30-minute anneal at 390°K

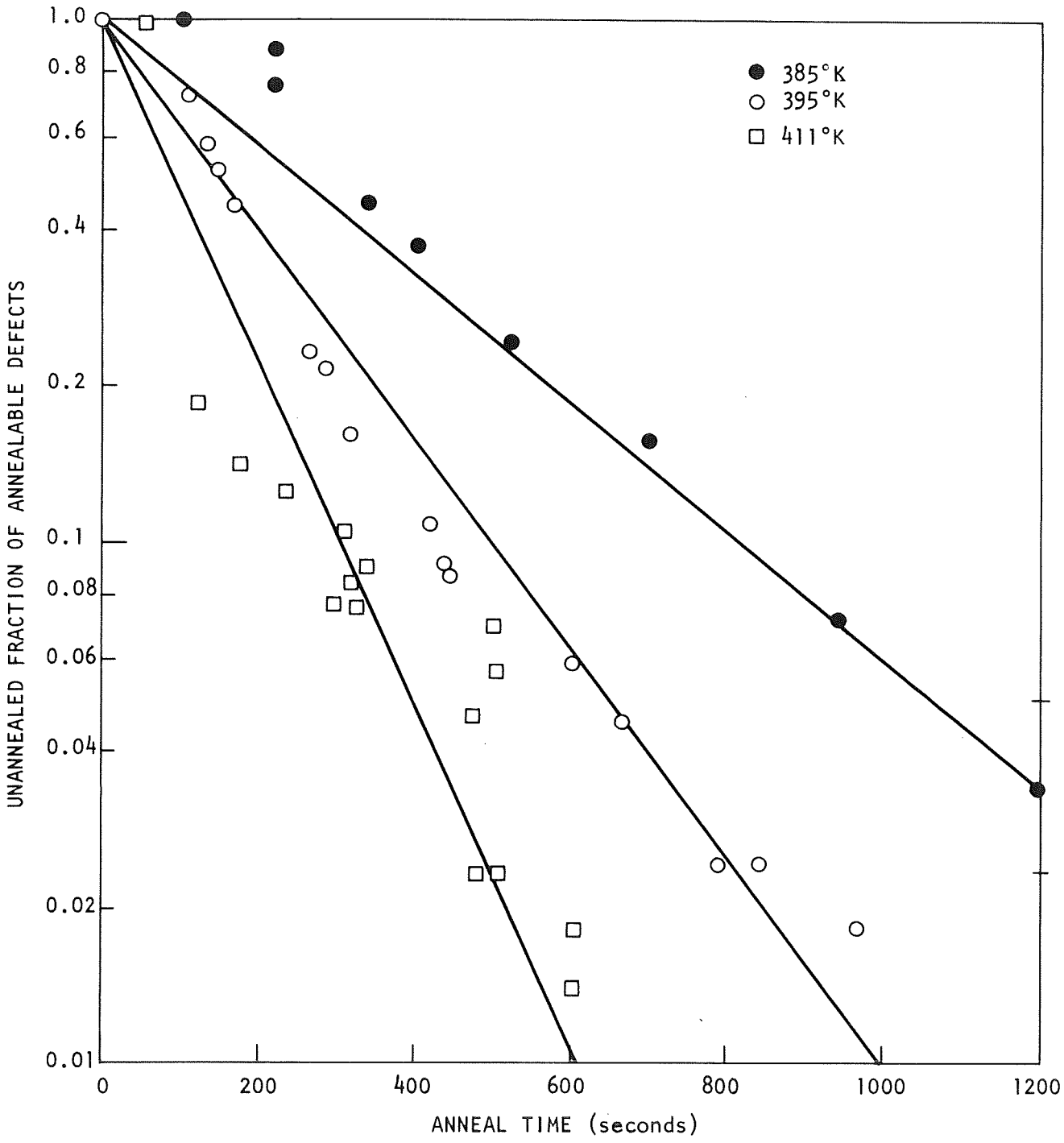

Fig. 5. Unannealed fraction of annealable recombination centers versus anneal duration for 385°, 395°, and 411°K anneals after 30-MeV electron irradiation at 300°K

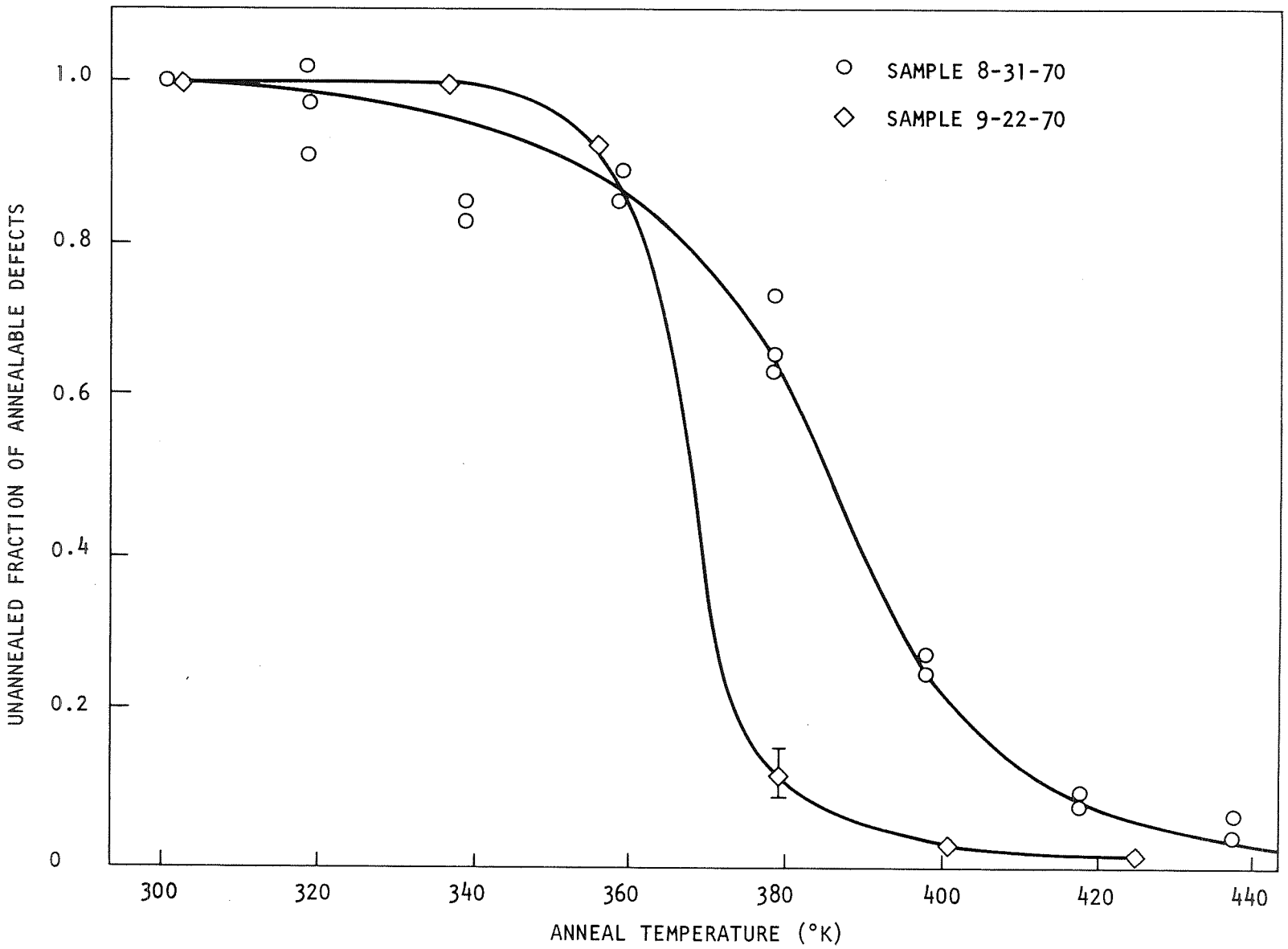

Fig. 6. Unannealed fraction of annealable defects for 5-minute isochronal anneals for 30-MeV electron-irradiated 2-ohm-cm lithium-diffused quartz-crucible silicon at 300°K

the positively charged Li^+ or LiO^+ donors rather than by the neutral oxygen present, and that the Si-Bl (oxygen-vacancy) is produced only when the number of mobile vacancies produced approaches or exceeds the number of Li^+ and LiO^+ donors initially present. This suggests that the observed deep radiation-induced center may be a lithium-vacancy or lithium-oxygen-vacancy.

Theoretical calculations indicate that one would expect about seven displaced atoms per incident 30-MeV electron. Since most of the vacancies produced never escape their interstitials, seven mobile vacancies per incident 30-MeV electron is a gross overestimate. However, in the present measurements, the lithium donor density is estimated to be $2 \times 10^{15}/cc$, and the total fluence to which the samples were exposed was $\varphi \simeq 1 \times 10^{13}$ e/cm^2. Thus, the lithium donor density exceeded the total number of displaced atoms by at least an order of magnitude.

The obvious experiment to test this hypothesis is to increase the total fluence or decrease the initial lithium donor density in order to see how the introduction rates of the Si-Bl center and the unidentified deep center depend on the ratio of electron fluence to lithium donor density.

One further remark would seem to be in order: In our previous investigations on the minority-carrier lifetime in lithium-diffused float-zone silicon, we observed a center located near E_c - 0.17 eV, which is about where one expects the Si-Bl center. We cannot definitely say this is not the Si-Bl center, nor have we otherwise identified this defect; however, the fact that a defect near E_c - 0.17 eV was observed in lithium-diffused float-zone (low-oxygen) silicon even before irradiation and not in lithium-diffused quartz-crucible (high-oxygen) silicon even after irradiation suggests that the center near E_c - 0.17 eV is probably not the Si-Bl center.

2.2 ELECTRON-SPIN RESONANCE

The study of paramagnetic defect centers produced by 30-MeV electron irradiations continued during this report period, with an annealing study. The characteristics of the samples studied are listed in Table 1.

Table 1

SAMPLES USED IN ESR STUDIES

Sample Number	Phosphorus Density/cc	Lithium Density/cc	Fluence (e/cm^2)	ESR Center	Introduction Rate (cm^{-1})
14	1.1×10^{16}	1.0×10^{16}	1.0×10^{17}	Si-G8	0.10
17	1.1×10^{16}	1.0×10^{16}	1.0×10^{17}	Si-G8	0.18
18	1.1×10^{16}	1.0×10^{16}	2.0×10^{17}	Si-G8	--
19	1.1×10^{16}	3.6×10^{16}	2.0×10^{17}	Si-G8	0.16
20	1.1×10^{16}	3.6×10^{16}	2.5×10^{17}	Si-G8	--

Figures 7 and 8 indicate the results of 15-minute isochronal anneals at elevated temperatures up to 673°K. Figure 7 indicates the change in room temperature resistivity, which is inversely proportional to carrier concentration, and Fig. 8 shows the change in concentration of paramagnetic centers. Figure 7 indicates a decreasing carrier concentration after 15-minute anneals up to about 373°K, followed by an increase after 15-minute anneals above 373°K.

The rapid increase in carrier concentration between 573° and 673°K in the 1:1, Li:P (sample 18) material, as opposed to the 3:1, Li:P (sample 20) material, might be due to the annealing of a lithium-related defect located below the Si-G8 (phosphorus-vacancy) level at 0.4 eV. In non-lithium-diffused silicon, the Si-G8 center anneals between 373° and 473°K; however, as indicated in Fig. 8, a large number of unidentified paramagnetic centers are still present after 15-minute anneals of from 473° to 673°K. Unfortunately, the resonance signal produced by these centers does not have enough structure to allow identification with our 9.2 Gc spectrometer.

In Fig. 7, the decreasing carrier concentration between 300° and 373°K could be due to the creation of acceptors below E_c - 0.4 eV. Such an increase was previously observed in a Si-B1 center study.[4] The increase in carrier concentration between 373° and 673°K is due to the annealing of the Si-G8 and perhaps other deeper centers. Since an absolute measure of the number of paramagnetic defects observed by ESR techniques is difficult, the defect densities in Fig. 8 were normalized to the known number of phosphorus atoms

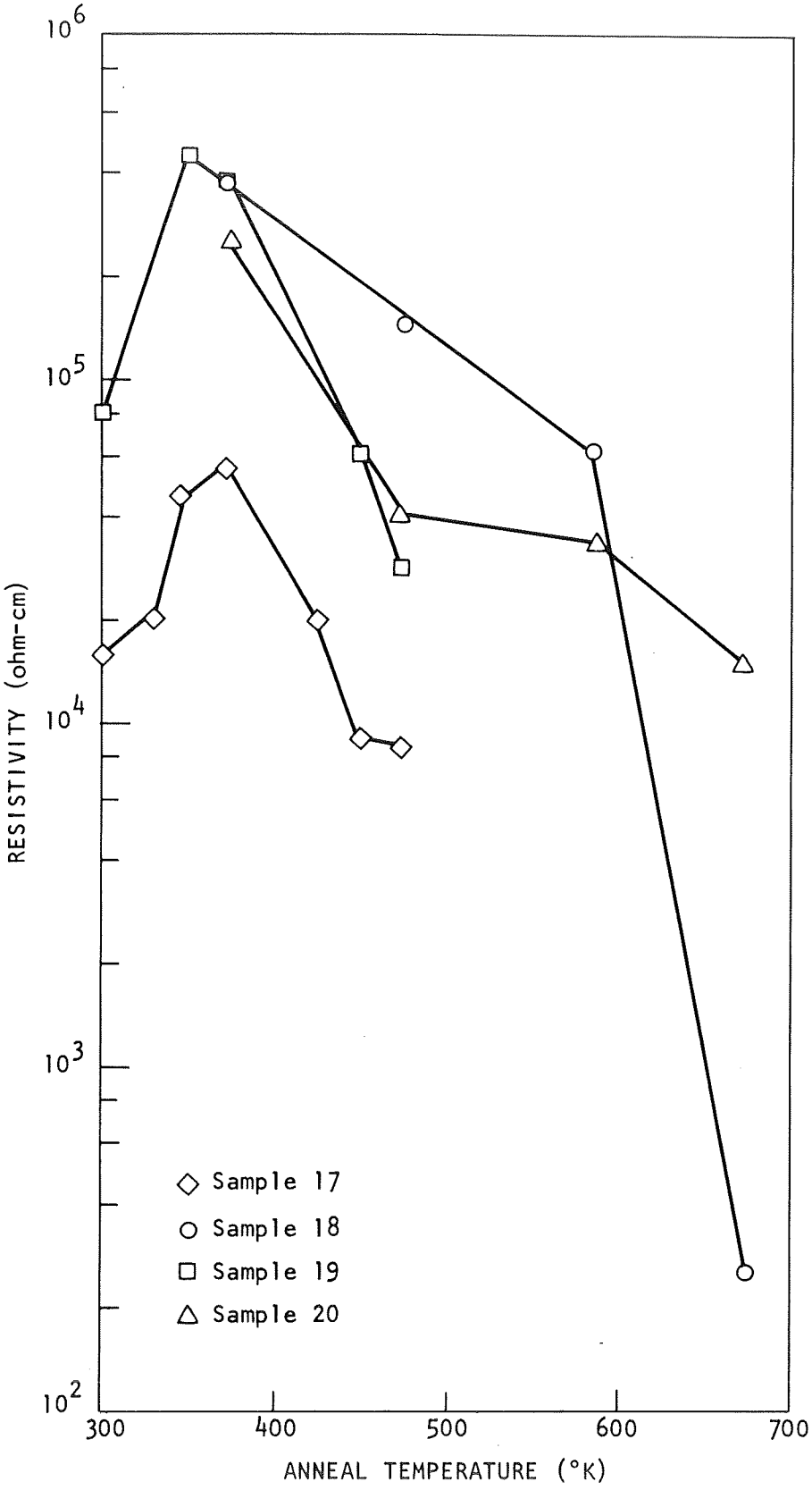

Fig. 7. Resistivity after 15-minute isochronal anneals for lithium-diffused electron-irradiated silicon

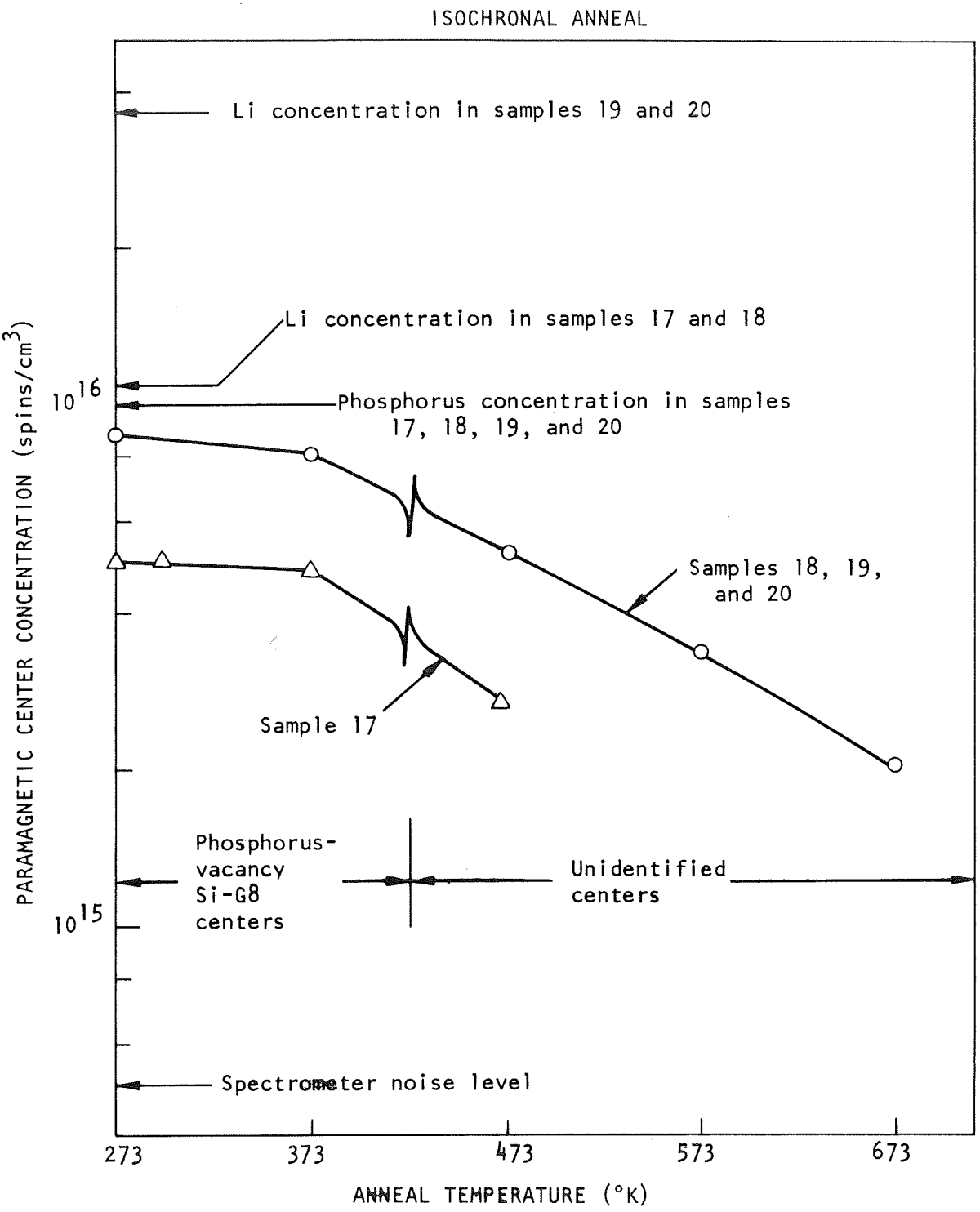

Fig. 8. Density of paramagnetic centers after 15-minute isochronal anneals for lithium-diffused phosphorus-doped electron-irradiated silicon

initially present in the sample (as determined by 4-probe resistivity measurements). This assumes that Si-G8 center production was in saturation at fluences of 2 x 10^{17} e/cm^2. The Si-G8 center introduction rate is believed to be approximately 0.1 cm^{-1} for 30-MeV electron irradiation.

During this reporting period, we made an observation which explains a previously unexplained observation that the phosphorus donor ESR signal was reduced by from 50 to 90% by the diffusion of lithium into phosphorus-doped silicon. A nonirradiated, lithium-diffused, phosphorus-doped sample of the same material used in preparation of all the ESR samples was examined for an LiO^+ resonance. A large resonance, with g = 1.999 and line width at half maximum of 1.9 gauss, was discovered, suggesting a LiO^+ density on the order of 10^{16} LiO^+/cm^3. This resonance, generally believed to be due to LiO^+, has the same g value as the marker that is used to calibrate the number of spins in the ESR samples.

This resonance signal is found only in the nonirradiated, lithium-diffused material, and its strength is about the same as the reference marker. Thus, a reexamination of previous data revealed that the apparent decrease in the phosphorus resonance upon lithium diffusion was actually due to an enhanced marker signal caused by the LiO resonance, and was not actually a decrease in the concentration of paramagnetic phosphorus donors.

2.3 INFRARED ABSORPTION STUDY OF DIVACANCY (Si-G7)

Infrared absorption bands at 1.8, 3.3, and 3.9 μm have been correlated with the divacancy.[6] The bands which are seen depend on the Fermi level position as shown by Fan and Ramdas.[7] Figure 9 indicates this dependence; the shaded areas indicate the range of Fermi level position over which each band is seen.

Two lithium-diffused optical samples and two nondiffused control samples were prepared from 10^4-ohm-cm float-zone silicon. The sample dimensions were 2 x 4 x 10 mm. The samples were diffused by the paint-on technique to a lithium donor density of about 5 x 10^{16} Li/cc. They were irradiated with 30-MeV electrons to a fluence of 2.5 x 10^{17} e/cm^2. The samples were immersed in liquid nitrogen during irradiation and their temperature never exceeded 150°K.

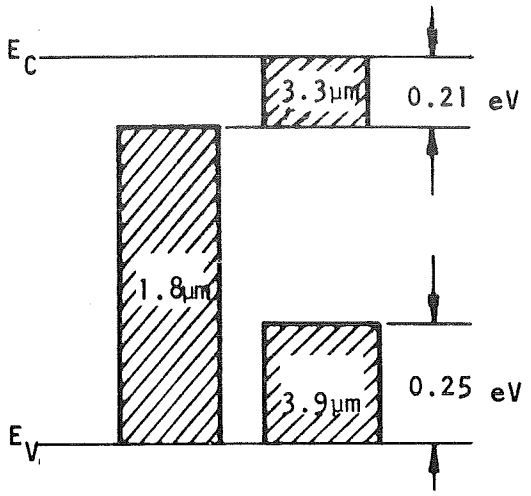

Fig. 9. Divacancy model

After irradiation, the samples were transferred (still at 77°K) to an optical dewar and optically scanned in a Perkin Elmer model 112 double-pass prism spectrometer in the 1.1- to 5-μm range. Both the diffused and the nondiffused samples showed comparable absorption in the 1.75- to 1.8-μm region, as shown in Fig. 10. This absorption is attributed to the divacancy when the Fermi level is below E_c - 0.21 eV.

In an effort to assure that no absorptions due to surface contamination were observed, the samples were warmed to room temperature and dried with dry nitrogen. On reexamination at 77°K, the 1.8-μm band in the lithium-diffused sample was found to be greatly reduced, and there was enhanced absorption near 1.4 and 1.65 μm. Annealing the samples below room temperature was impossible with the equipment being used. The samples were then warmed to room temperature again and immediately examined in the 1.1- to 2.5-μm region. After less than 30 minutes at 300°K, the 1.8-μm band had virtually disappeared in the lithium-diffused sample and bands near 1.4 and 1.65 μm had appeared. These bands have previously been observed by Young et al.[8] in lithium-diffused silicon. The primary difference between this investigation and Young's is that Young irradiated near 300°K rather than near 150°K; hence, the 1.8-μm divacancy band he observed was considerably less dense than the one we observed. Young's samples had undergone 300°K annealing before his measurements commenced. Our samples were isochronally annealed for 15-minute periods in 50°C steps from ~400° to ~625°K. The results of this anneal are substantially in agreement with those of Young et al.

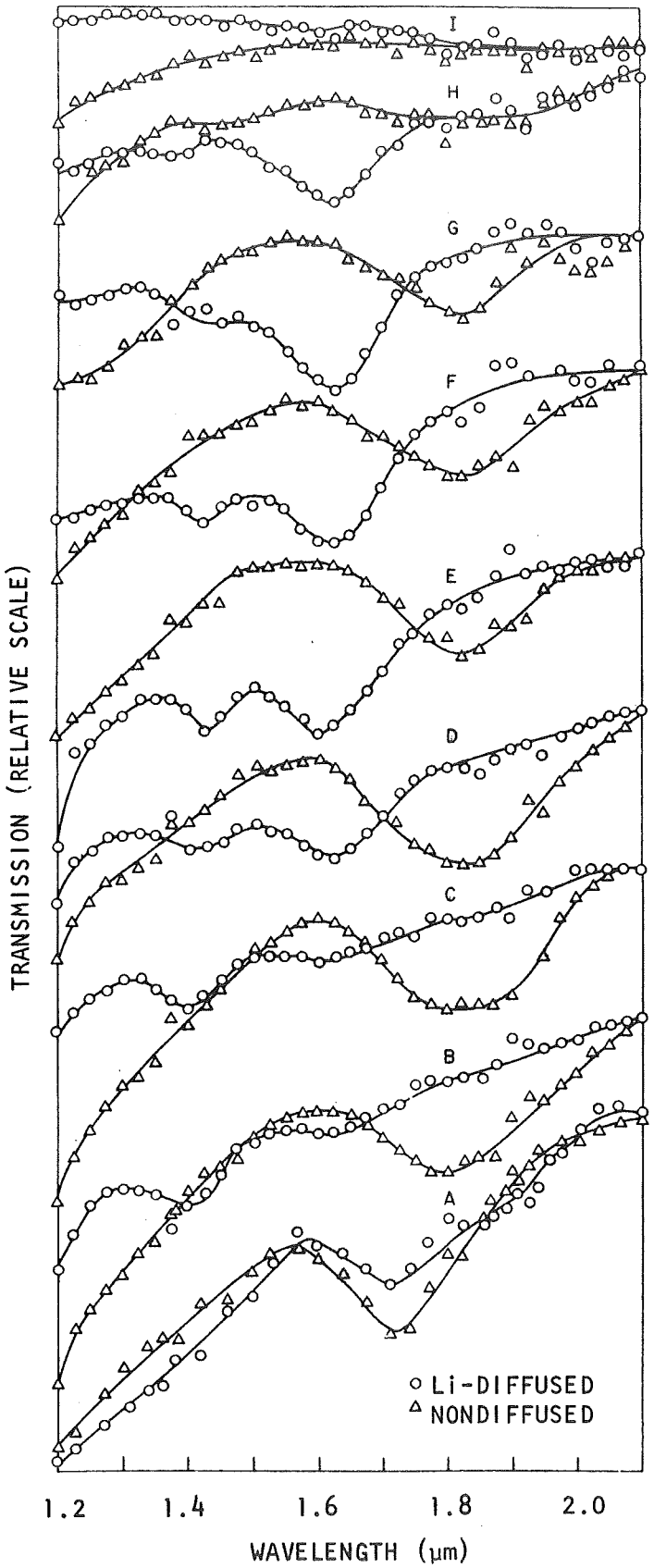

Fig. 10. Relative transmission of high-purity FZ (10^4 ohm-cm) and high-purity lithium-diffused (n_{O_2} = 5 x 10^{16} Li/cc) FZ silicon after irradiation with 2.5 x 10^{17} e/cm^2 (30 MeV) at less than 150°K. Curves A and B are normalized to the tungsten light source, while the other curves are normalized to transmission through a 10^4 ohm-cm nonirradiated sample. The history of the samples is given in Table 2.2. Resolu- is better than 0.02 μm.

Young et al. attribute the 1.4- and 1.65-μm bands to defect complexes consisting of one and two Li^+ ions, respectively, which are trapped by a divacancy.

It is clear from Fig. 10 that the Si-G7 anneals at much lower temperature in lithium-diffused silicon than in non-lithium-diffused silicon; in nondiffused silicon, it anneals near 625°K.

Table 2 lists presents the annealing history of the samples used in the divacancy study.

Table 2

ANNEALING HISTORY OF SAMPLES USED IN DIVACANCY STUDY

Curve Designation	Sample Temperature	Anneal Temperature	Anneal Duration
A	77°K	<150°K	Intermittent during irradiation
B	300°K	300°K	< 30 minutes
C	300°K	300°K	12 hours
D	300°K	398°K	15 minutes
E	300°K	448°K	15 minutes
F	300°K	473°K	15 minutes
G	300°K	523°K	15 minutes
H	300°K	573°K	15 minutes
I	300°K	623°K	15 minutes

3. COMPUTER SIMULATION

3.1 INTRODUCTION

During this period, it was decided that questions raised by runs done to date lead to two more or less separate sets of experiments. The first is one in which the cell is kept as simple as possible—step junction, uniform generation level, uniform lifetimes but with a high recombination region at the boundary to simulate a boundary condition of zero excess carrier density. These parameters will then be varied to verify whether we understand how important physical parameters determine the electrical characteristics of the cell. Initial stages of this experiment as well as various theoretical considerations of the open circuit voltage V_{oc} are given in Section 3.3.

The second experiment is to see whether the parameters can be varied to bring the computed I-V curve to more exact agreement with the curve we have adopted as a prototype. This is the subject of Section 3.4.

Section 3.2 discusses the way the lifetimes are selected for use in the PN code.

3.2 RECOMBINATION LIFETIMES

The recombination rate in the PN code is the Shockley-Read[10] expression

$$R = \frac{(np - n_i^2)}{\tau_{no}\,(p + p_F) + \tau_{po}\,(n + n_F)}\,, \qquad (1)$$

where n_i is the intrinsic carrier density, 1.4×10^{10} cm^{-3} in silicon. The densities p_F and n_F are the carrier densities if the Fermi level were at the recombination energy level E_R measured from the conduction band. We assume nondegeneracy and use

$$n_F = N_c\, e^{-E_R/kT}\,, \qquad (2)$$

where N_c is the effective density of states, which is 2.79×10^{19} cm^{-3} in silicon at room temperature. The hole density is then found from the law of mass action:

$$p_F = n_i^2/n_F \ . \tag{3}$$

The term lifetime will be used subsequently to mean the low injection level lifetimes appearing in Eq. 1.

$$\tau_{no} = 1/(v_n \sigma_n N) \ , \tag{4a}$$

$$\tau_{np} = 1/(v_p \sigma_p N) \ . \tag{4b}$$

In Eq. 4, N is the density of recombination centers, v is the thermal velocity, and σ is the capture cross section. A nominal value of 10^7 cm/sec is used for v_p, and the velocity v_n is then found from

$$v_n = v_p \sqrt{m_p/m_n} = 0.82 \ v_p \ . \tag{5}$$

The specific value 0.82 is obtained from the density-of-states masses. The value of the cross sections, σ, depends on whether the center is charged or neutral for that particular capture. In fact, near room temperature the two cross sections appear to differ very little[11] and, for the following, we have assumed them both to be equal to 5×10^{-16} cm^2, in which case the lifetimes will differ only by the ration 0.82 of Eq. 5.

3.3 VALUE OF OPEN CIRCUIT VOLTAGE

The short circuit current, I_{sc}, is universally attributed to the diffusion length; see, for example, Eq. 3 of Wysocki and Rappaport.[12]

$$I_{sc} = qg \ (L_n + L_p) \ , \tag{6}$$

where q is the electronic charge, g is the uniform generation rate, and

$$L = \sqrt{D\tau} \ , \tag{7}$$

where D is the diffusion constant and τ is the lifetime. In Eq. 6, the

diffusion lengths that enter are for the side where that carrier is the minority: L_n from the p side, L_p from the n side. Reference 12 also gives V_{oc} as

$$V_{oc} = kT \log (I_{sc}/I_o + 1) , \tag{8}$$

where I_o is the diode saturation current,

$$I_o = qn_i^2 (L_n/\tau_n N_A + L_p/\tau_p N_D) . \tag{9}$$

According to Eq. 8, V_{oc} will increase as I_o decreases, so N_D, the doping on the n side, should be made large; but this tack becomes of no avail as soon as N_D is increased to the point where the first term is larger than the second. At this point, the doping of the base material, N_A, must be increased.

Another estimate of the open circuit voltage can be made by arguing that the electron density in the base region, $g\tau_n$, will fill the conduction band up to an energy E_p given by

$$g\tau_n = N_c e^{(E_p - \eta_p)/kT} , \tag{10}$$

where η_p is the Fermi level on the p side. The density of electrons in the n region, N_D, must satisfy an analogous relation

$$N_D = N_c e^{(E_n - \eta_n)/kT} . \tag{11}$$

An expression relating the energies is found by dividing Eq. 10 by Eq. 11 to find

$$g\tau_n/N_D = \exp [(E_p - E_n + \eta_n - \eta_p)/kT] . \tag{12}$$

The difference in Fermi levels represents the energy gained by transferring a single electron from one side to the other; i.e., it is V_{oc}:

$$V_{oc} = \eta_n - \eta_p . \tag{13}$$

The two populations of electrons, while not in thermodynamic equilibrium (if they were, $\eta_n = \eta_p$), are free to exchange electrons across the junction,

so they must both reach the same energy level when that level is referred to the same zero. This is illustrated in Fig. 11. The bottom of the band on the n side is lowered by the built-in voltage, V_b:

$$E_p = E_n - V_b \ . \tag{14}$$

The use of Eqs. 13 and 14 in Eq. 12 yields

$$V_{oc} = V_b + kT \log (g\tau_n/N_D) \ . \tag{15}$$

Note that $g\tau_n/N_D$ is less than one for all practical cases, so V_{oc} is less than V_b. (Equation 15 must become invalid as $g\tau_n/N_D$ approaches unity because V_{oc} can never exceed V_b.)

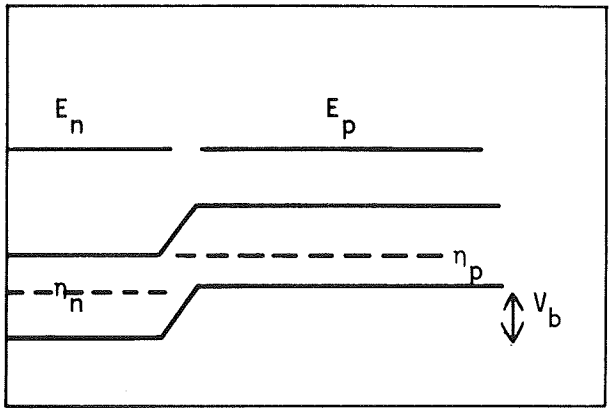

Fig. 11. Diagram showing the relative energies of carriers across an n/p solar cell junction

A limited test of Eq. 15 was made during this reporting period, with parameters as shown in Table 3. The values of V_{oc} computed by Eq. 15 are identical to the values computed from Eq. 8. These are compared to values of V_{oc} obtained from the PN code in Fig. 12. It is intended to obtain I_{sc} for this case and to vary the lifetime and doping level to check in more detail our understanding of how the physics behind the cell operation determines the efficiency and maximum power output. This, in turn, will help us understand how the power is degraded as the cell parameters are modified by radiation.

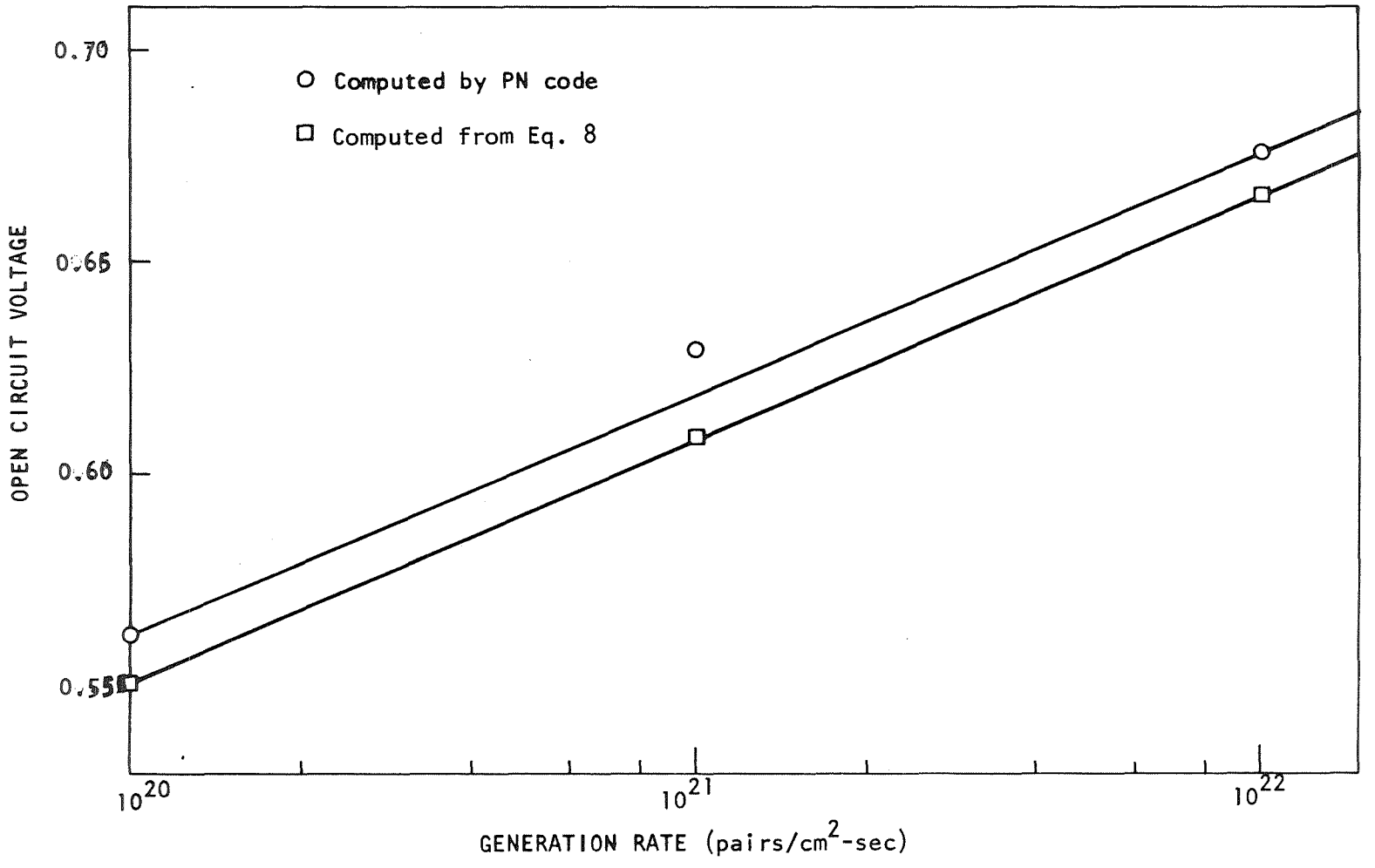

Fig. 12. V_{oc} versus g for run 310.1; N = 10^{18} cm^{-3}, τ = 5 μsec, kT = 0.025 eV (nominal value for room temperature); built-in voltage 0.74165; 10-ohm-cm base material

Table 3

STEP JUNCTION, PROBLEM 310.1 TO EXPLORE V_{oc}

	Doping (cm^{-3})	τ (sec)	L (cm)	$L/N\tau$ (cm^4/sec)
N side	10^{18}	2.5×10^{-9}	1.2×10^{-4}	4.8×10^{-14}
P side	1.5×10^{15}	5.0×10^{-6}	1.2×10^{-2}	1.6×10^{-12}

3.4 CONSTRUCTION OF A RUN TO OBTAIN A SPECIFIC I-V CURVE

The previous runs, such as reported in Fig. 7, p. 16 of Ref. 13, have had a V_{oc} somewhat smaller than the prototype curve and an I_{sc} somewhat larger. In constructing a new run to effect changes in the correct direction, it was also decided to employ a doping profile that is more realistic than the step used previously. The profile selected was a complimentary error function such as would be obtained by holding the donor concentration at the front surface equal to 10^{19} cm^{-3} long enough to diffuse a junction to a depth of 1/2 μm. The lifetimes in the n region were chosen by supposing that the donors act as the dominant recombination center. Thus, N is equal to N_D in Eq. 4; this results in lifetimes that vary from 10^{-11} sec at the surface to about 10^{-7} sec at the junction. A phosphorus donor has an energy level E_R of E_c - 0.45 eV. Equation 2 then yields an n_F of 4.7×10^{18} cm^{-3}. In the base, a 10-ohm-cm material with $N_A = 1.5 \times 10^{15}$ cm^{-3} is again used. It was estimated that the current should be decreased somewhat. Equations 6 and 7 state that this can be done by decreasing the lifetime. The value of τ_n in the base region was taken to be 1.3 μsec. The base region recombination center is assumed to be near the middle of the band gap, with $n_F \simeq 1.4 \times 10^{10}$ cm^{-3}.

The I-V curve generated by this new cell (called problem No. 706.1) is shown in Fig. 13. Its current I_{sc} is larger and its V_{oc} smaller than the desired values. On the basis of run 706.1, it appears that very good agreement will be achieved by lowering the lifetime in the base to decrease I_{sc}, and by increasing the doping in the base to increase V_{oc}. In the latter case, we assume that the base material resistivity is actually somewhat lower than its nominal value of 10 ohm-cm.

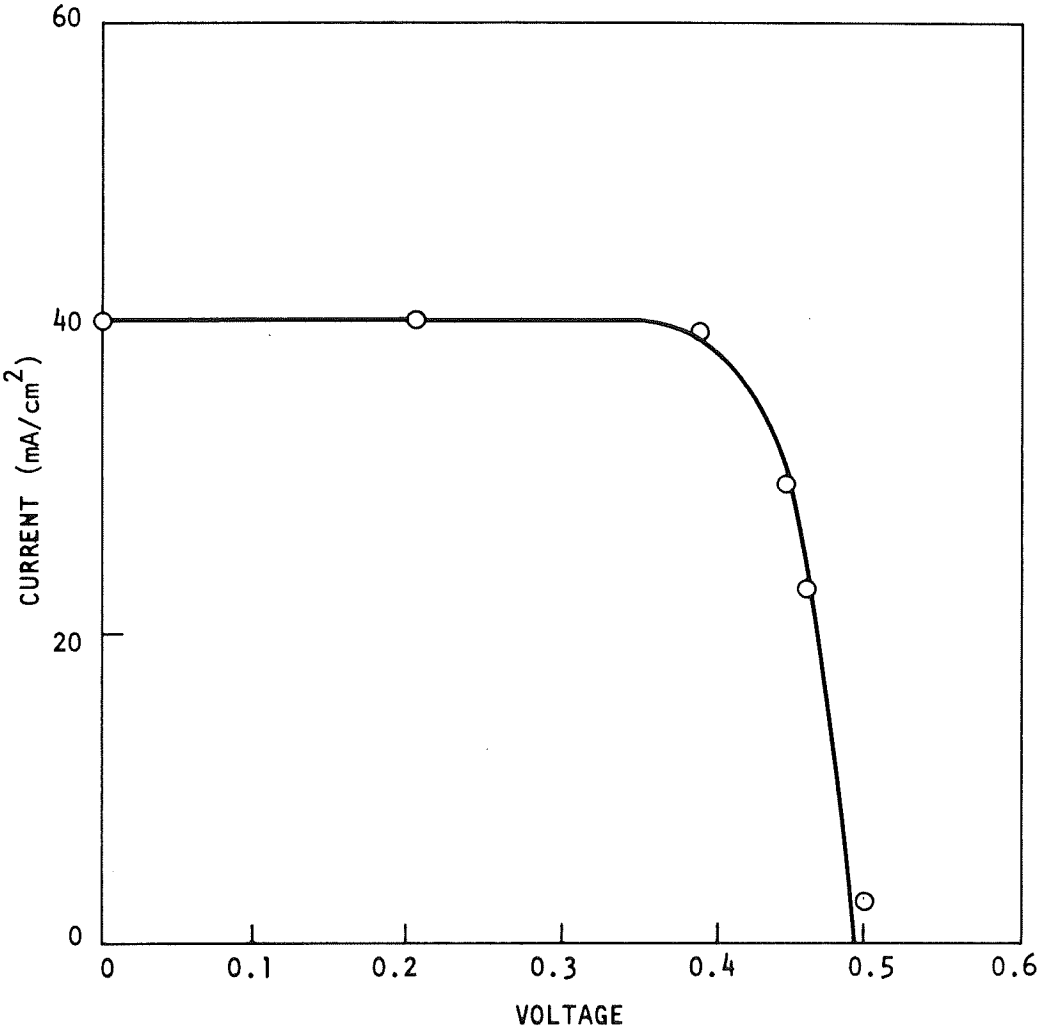

Fig. 13. Computer-generated solar cell I-V output for run 706.1 (cell parameters are described in text)

4. PLANS FOR THE NEXT REPORTING PERIOD

Minority-carrier lifetime studies of lithium-diffused crucible-grown silicon will continue. Emphasis will be placed on lifetime temperature dependence of electron-irradiated lithium-diffused quartz-crucible silicon and annealing kinetics. Particular attention will be paid to the effect of lithium on the production and anneal of Si-Bl centers. A neutron irradiation is planned as soon as time on the accelerator pulsed fast assembly (APFA) is assigned. Computer simulation of solar cell characteristics will continue.

5. NEW TECHNOLOGY

No new technology is currently being developed or employed in this program.

6. PUBLICATIONS

During this period, papers describing work performed under this contract were presented by J. A. Naber at the 1970 International Conference on Radiation Effects in Semiconductors at the State University of New York, and by B. C. Passenheim at the Eighth Photovoltaic Specialists Conference, Seattle.

7. SUMMARY

Work on minority-carrier lifetime, electron-spin resonance, studies of lithium-diffused silicon, and computer simulation of solar cell outputs has continued. Partial results of the investigations performed under this contract were presented at two conferences.

REFERENCES

1. M. Lax, Phys. Rev. 119, 1502 (1960).

2. J. C. Irvin, Bell System Tech. J. XLI, 387 (1962).

3. J. W. Corbett, R. W. McDonald, and G. D. Watkins, J. Phys. Chem. Solids 25, 873 (1964).

4. J. A. Naber, H. Horiye, and V. A. J. van Lint, "Radiation Effects in Silicon," Gulf Rad Tech report GA-8668, 20 August 1968.

5. R. E. Leadon, J. A. Naber, and T. M. Flanagan, "Research on the Physics of Transient Radiation Effects," Gulf Rad Tech report GA-9334, April 1969.

6. L. J. Cheng et al., Phys. Rev. 152, 761 (1966).

7. H. Y. Fan and A. K. Ramdas, J. Appl. Phys. 30, 1127 (1959).

8. R. C. Young et al., J. Appl. Phys. 40, 271 (1969).

9. F. L. Vook and H. J. Stein, "Production of Defects in N-Silicon," published in Radiation Effects in Semiconductors, F. L. Vook, ed., Plenum Press, New York, 1968.

10. W. Shockley and W. T. Read, Phys. Rev. 87, 835 (1952).

11. R. Cesena et al., "Research on the Physics of Transient Radiation Effects," Gulf Rad Tech report GA-10098, April 1970.

12. J. J. Wysocki and P. Rappaport, J. Appl. Phys. 31, 571 (1960).

13. B. C. Passenheim et al., "Radiation Effects in Silicon Solar Cells," Quarterly Progress Report (April 1 - June 30, 1970) on contract JPL-952387, Gulf Rad Tech report GA-10219, July 10, 1970.